

Supplemental Materials

Molecular Biology of the Cell

Somasundarama and Taraska

Supplemental Figure 1. Frequency of microvesicle fusion events, and radial spread of VACHT-pH following exocytosis, in PC12 cells. (A) Histogram showing number of fusion events before and after application of stimulation buffer (KCl). (B) Average normalized radial line scans of VACHT-pH during fusion. Contrast has been adjusted to show areas with lower intensity. Vertical dotted lines indicate the time-points corresponding to linescan intensity plots (Right). Standard errors are plotted as shaded areas around the average traces. Data was obtained from cells co-expressing VACHT-pH and farnesyl-mCherry. (C) Average time-lapse traces of normalized fluorescence intensities for VACHT-pHuji (magenta) and NPY-GFP (green). Individual event traces were time-aligned to 0 s, which corresponds to the fusion frame in the red channel. Standard errors are plotted as shaded areas around the average traces. (D) List of plasmids, sources of cDNA, and the number of events and cells analyzed for each protein. *Truncated CMV promoter.

Supplemental Figure 2. Dynamics of Rab proteins during SLMV fusion. (A) Average normalized radial line scans of the Rab proteins during microvesicle exocytosis. Bar, 1 μm . Vertical dotted lines indicate the time-points corresponding to linescan intensity plots (Right). Standard errors are plotted as shaded areas around the average traces.

Supplemental Figure 3. Dynamics of SNARE proteins during fusion. (A) Average normalized radial line scan analysis of SNAREs and control mCherry proteins during microvesicle exocytosis. Bar, 1 μm . Vertical dotted lines indicate the time-points corresponding to linescan intensity plots (Right). Standard errors are plotted as shaded areas around the average traces.

Supplemental Figure 4. Synaptotagmin1 and Muncprotein behavior at SLMV fusion sites. (A-C) Average time-lapse traces of normalized fluorescence intensities for: (A) synaptotagmin1-mCherry (266 events, 5 cells), (B) mCherry-Munc18a (250 events, 11 cells), and (C) Munc13-mCherry (132 events, 5 cells). Individual event traces were time-aligned to 0 s (vertical black line), which corresponds to the fusion frame in the green channel. Standard errors are plotted as shaded areas around the average traces. * $p \leq 0.05$, ns – not significant, when compared with baseline.

Supplemental Figure 5. Dynamics of SNARE modulators during SLMV fusion. (A) Average normalized radial line scans of accessory proteins during microvesicle exocytosis. Bar, 1 μm . Vertical dotted lines indicate the time-points corresponding to linescan intensity plots (Right). Standard errors are plotted as shaded areas around the average traces.

Supplemental Figure 6. Dynamics of WT and mutant amphiphysin1 and syndapin2, and diffusion of VACHT-pH, during SLMV fusion. (A) Average normalized radial line scans of WT and mutant amphiphysin1 and syndapin2 proteins during microvesicle exocytosis. Bar, 1 μm . (B) Average normalized radial line scans of VACHT-pH during fusion in PC12 cells co-expressing syndapin2-BAR. Contrast has been adjusted to show areas with lower intensity. Vertical dotted lines indicate the time-points corresponding to linescan

intensity plots (Right). Standard errors are plotted as shaded areas around the average traces.

Supplemental Figure 7. Endophilins are localized at SLMV fusion sites during exocytosis. (A-C) (Left) Average time-lapse traces of normalized fluorescence intensities for: (A) endophilinA1-mCherry (258 events, 13 cells), (B) endophilinA2-mCherry (207 events, 11 cells), and (C) endophilinB1-mCherry (213 events, 11 cells). Individual event traces were time-aligned to 0 s (vertical black line), which corresponds to the fusion frame in the green channel. * $p \leq 0.05$, ** $p \leq 0.01$, *** $p \leq 0.0001$, ns – not significant, when compared with baseline. (Middle) Average normalized radial line scans of endophilins during fusion. Bar, 1 μm . Vertical dotted lines indicate the time-points corresponding to linescan intensity plots (Right). Standard errors are plotted as shaded areas around the average traces.

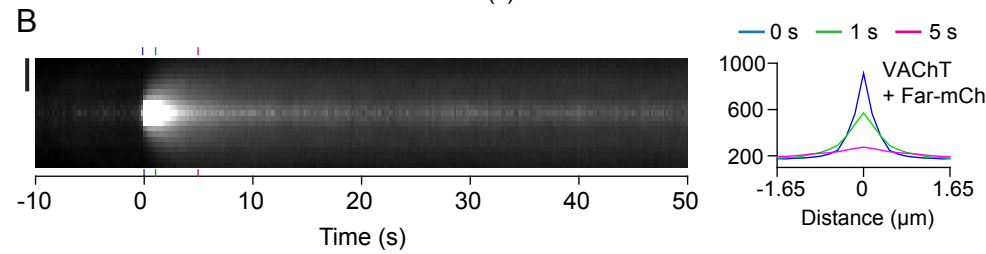
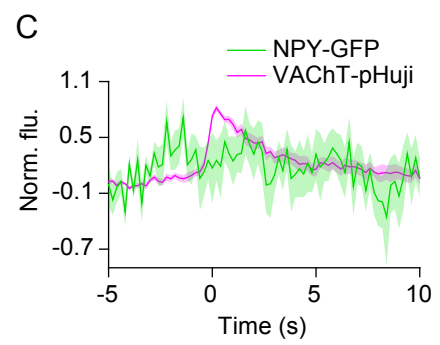
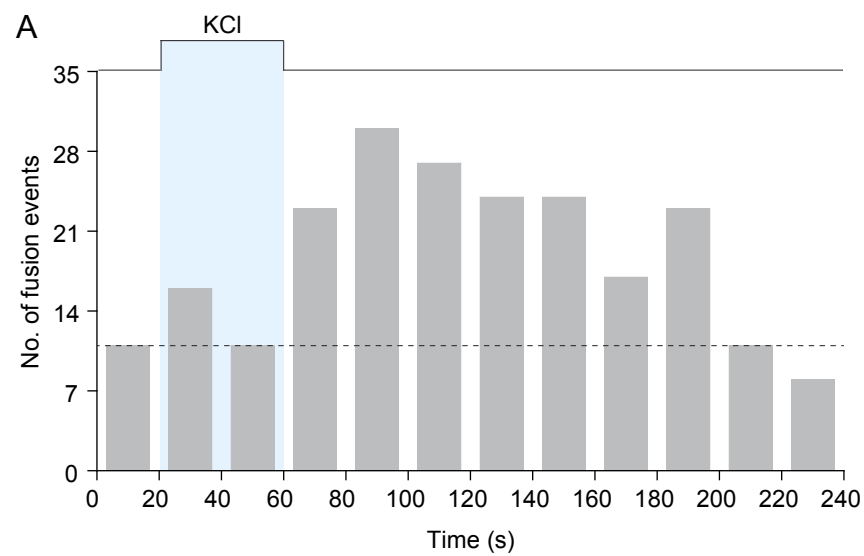
Supplemental Figure 8. Effect of BAR domain proteins on loss of VACHT-pH from SLMV fusion sites. (A-D) Average time-lapse traces of normalized VACHT-pH fluorescence intensities in cells co-expressing VACHT-pH and the indicated BAR domain or control mCherry proteins. Individual traces were time-aligned to 0 s, which corresponds to the frame of fusion. Standard errors are plotted as shaded areas around the average traces.

Supplemental Figure 9. Effect of syndapin2 knock-down on VACHT-pH loss from fusion sites. (A) Western blots showing expression of syndapin2 in PC12 cells, that is reduced following treatment with siRNA. (Top) Blot probed with anti-syndapin2 antibody. (Bottom) Same blot re-probed with anti- α -actin. (B) Average time-lapse traces of normalized VACHT-pH fluorescence intensities in cells treated with control siRNA (219 events, 15 cells) or sisyndapin2 (184 events, 16 cells). Individual traces were time-aligned to 0 s, which corresponds to the fusion frame. Standard errors are plotted as shaded areas around the average traces.

Supplemental Figure 10. Recruitment of WT and mutant dynamin to SLMV fusion sites, and effect of BAR domain proteins and dynamin on VACHT decay. (A-F) (Left) Average time-lapse traces of normalized fluorescence intensities for: (A) Dynamin1-WT (250 events, 14 cells), (B) Dynamin-K44A (309 events, 12 cells), (C) Dynamin1- Δ Amph1 (365 events, 17 cells), (D) Dynamin1- Δ Synd2 (341 events, 17 cells), (E) Dynamin2-WT (260 events, 12 cells), and (F) Dynamin2- Δ PRD (252 events, 14 cells). Individual event traces were time-aligned to 0 s (vertical black line), which corresponds to the fusion frame in the green channel. * $p \leq 0.05$, ** $p \leq 0.01$, *** $p \leq 0.0001$, ns – not significant, when compared with baseline. (Middle) Average normalized radial line scans of WT and mutant dynamin proteins during microvesicle exocytosis. Bar, 1 μm . Vertical dotted lines indicate the time-points corresponding to linescan intensity plots (Right). Standard errors are plotted as shaded areas around the average traces. (G) Single exponential decay constants for VACHT-pH when co-expressed with the indicated constructs, or treated with the indicated siRNA.

Supplemental Figure 11. Dynamics of other endocytic proteins at SLMV fusion sites. (A-D) (Left) Average time-lapse traces of normalized fluorescence intensities for: (A) N-WASP-mCherry (197 events, 8 cells), (B) ClathrinLC-mCherry (209 events, 5 cells), (C) AP2- μ 2-mCherry (153 events, 5 cells), and (D) mCherry-Intersectin (122 events, 5 cells). Individual event traces were time-aligned to 0 s (vertical black line), which corresponds to the fusion frame in the green channel. * $p \leq 0.05$, ** $p \leq 0.01$, ns – not significant, when compared with baseline. (Middle) Average normalized radial line scan analysis. Bar, 1 μ m. Vertical dotted lines indicate the time-points corresponding to linescan intensity plots (Right). Standard errors are plotted as shaded areas around the average traces.

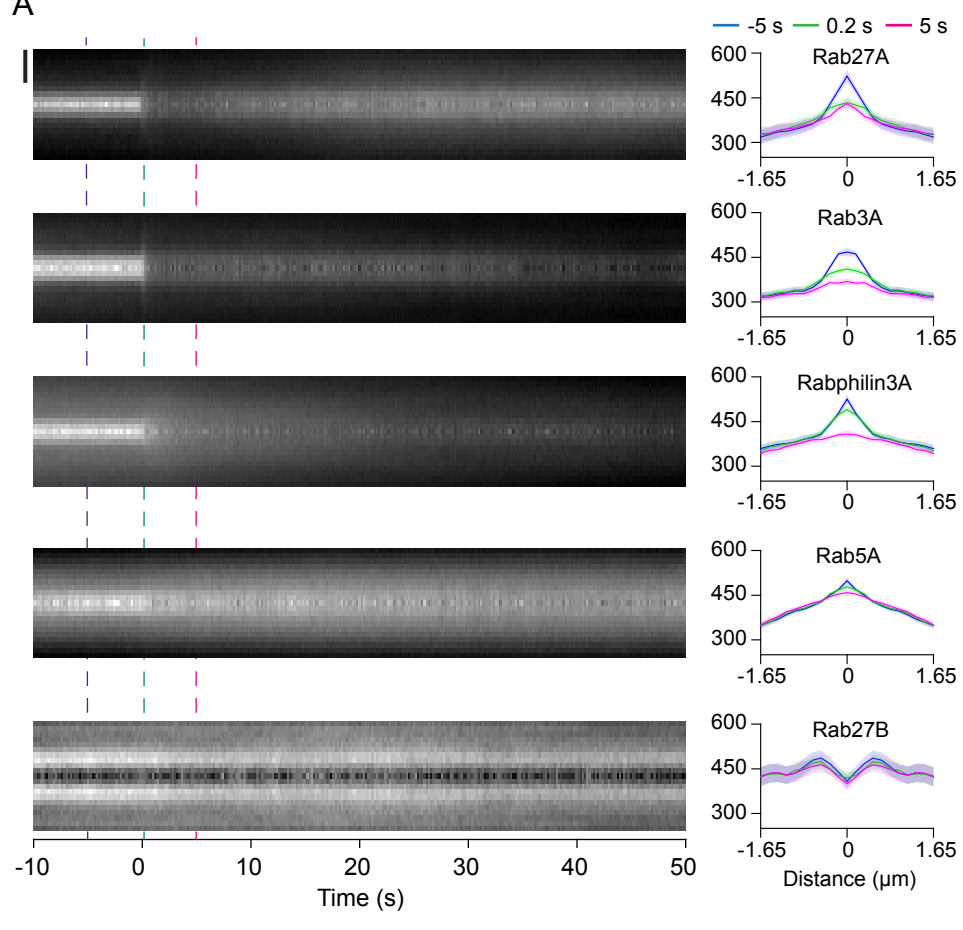
Supplemental Figure 12. Plasma membrane recruitment of amphiphysin1 following stimulation. (A) Images of a PC12 cell expressing VAcHT-pH (top) and Amph1-mCherry (bottom) at indicated time-points, with '0 s' being the start of the experiment. Stimulation buffer (KCl) was applied from ~ 20 s to 60 s. Bar, 5 μ m. (B) Time-lapse traces show background-subtracted and normalized mean fluorescence intensities for VAcHT-pH (green) and amphiphysin1-mCherry (magenta) from a region around the whole cell.



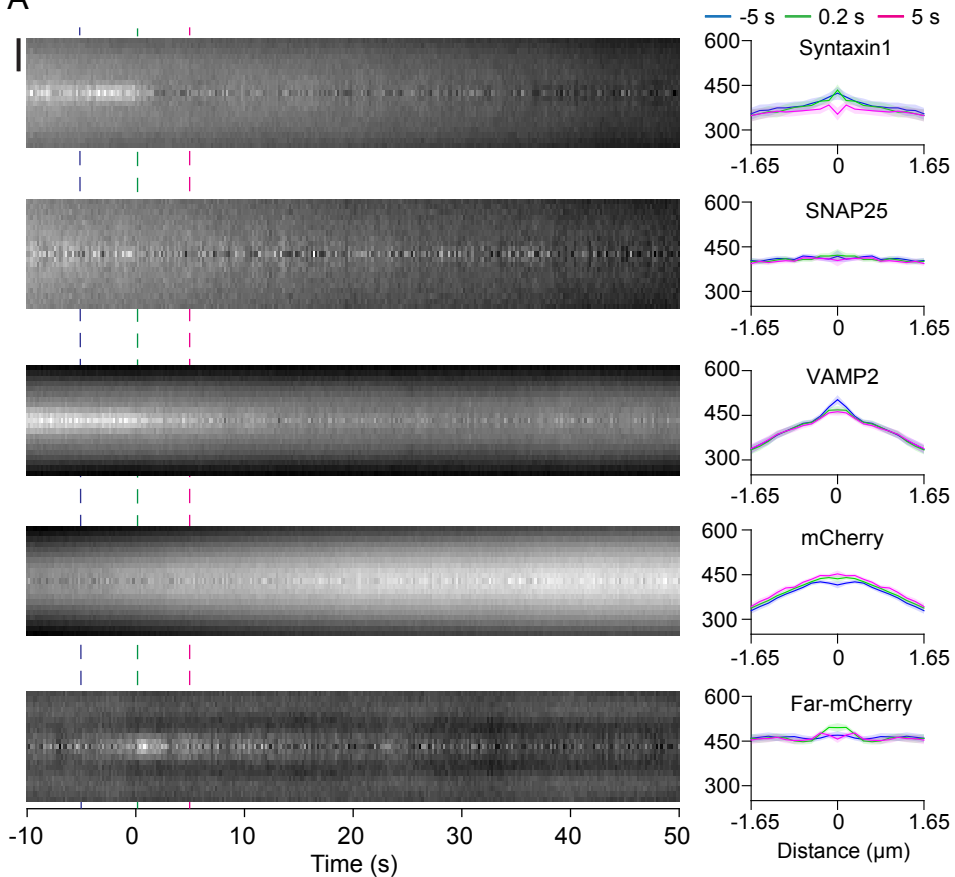
D

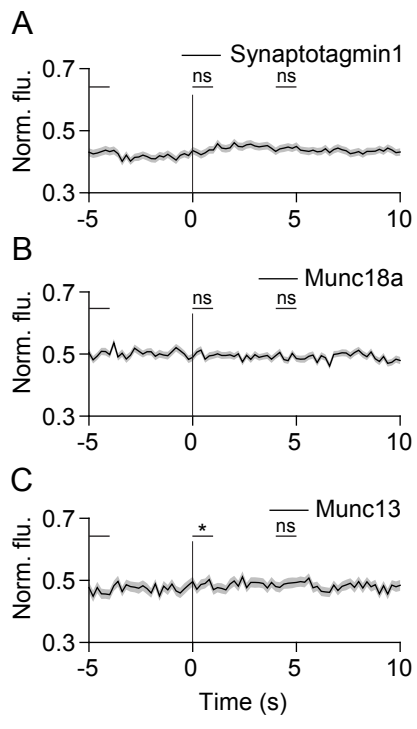
DNA Construct	No. of Events	No. of Cells	Source of cDNA
VAcHT-pHluorin			D. Clapham (Janelia)
dCMV-mCherry-Syntaxin1a*	76	4	W. Almers (OHSU)
dCMV-mCherry-SNAP25*	97	8	J. Taraska (NHLBI/NIH)
VAMP2-mCherry	172	7	R. Scheller (Stanford U.)
mCherry	274	8	Clontech
Farnesyl-mCherry	166	9	J. Taraska (NHLBI/NIH)
Complexin2-mCherry	202	7	Biobasic synthesis
CAPS-mKate2	232	5	T. Martin (UW, Madison)
mCherry-Tomosyn	289	9	Biobasic synthesis
NSF-mCherry	274	5	P. Hanson (Wash U.)
Synaptotagmin1-mCherry	266	5	J. Taraska (NHLBI/NIH)
mCherry-Munc18a	250	11	Biobasic synthesis
Munc13-mCherry	132	5	Biobasic synthesis
mCherry-Rab27A	103	4	W. Westbroek (NIH)
mRFP-Rab3A	196	5	M. Fukuda (Tohoku U.)
mCherry-Rabphilin3A	198	6	I. Macara (Vanderbilt U.)
mCherry-Rab5A	276	6	C. Merrifield (Addgene 27681)
mCherry-Rab27B	73	3	J. Taraska (NHLBI/NIH)
Amphiphysin1-mCherry	371	9	C. Merrifield (Addgene 27692)
Amphiphysin1- Δ BAR-mCherry	169	4	J. Taraska (NHLBI/NIH)
Amphiphysin1- Δ SH3-mCherry	214	13	J. Taraska (NHLBI/NIH)
Amphiphysin1-SH3-mCherry	117	8	J. Taraska (NHLBI/NIH)
mCherry-Syndapin2	228	6	C. Merrifield (Addgene 27681)
mCherry-Syndapin2- Δ BAR	136	11	J. Taraska (NHLBI/NIH)
mCherry-Syndapin2-BAR	418	13	J. Taraska (NHLBI/NIH)
mCherry-Syndapin2- Δ SH3	184	9	J. Taraska (NHLBI/NIH)
EndophilinA1-mCherry	258	13	DNASU HsCD00000899
EndophilinA2-mCherry	207	11	DNASU HsCD00005501
EndophilinB1-mCherry	213	11	DNASU HsCD00042012
Dynamin1-mCherry	250	14	C. Merrifield (Addgene 27697)
Dynamin1-K44A-mCherry	309	12	J. Taraska (NHLBI/NIH)
Dynamin1-833-838A-mCherry	365	17	J. Taraska (NHLBI/NIH)
Dynamin1-S774E/S778E-mCherry	341	17	J. Taraska (NHLBI/NIH)
Dynamin2-mCherry	260	12	C. Merrifield (Addgene 27689)
Dynamin2- Δ PRD-mCherry	252	14	J. Taraska (NHLBI/NIH)
mCherry-N-WASP	197	8	H. Yamada (Okayama U.)
AP2- μ 2-mCherry	153	5	C. Merrifield (Addgene 27672)
mCherry-Intersectin	122	5	Peter McPherson (McGill U.)
Clathrin Light Chain-mCherry	209	5	W. Almers (OHSU)
Total	8249	324	
Average	217.08	8.53	

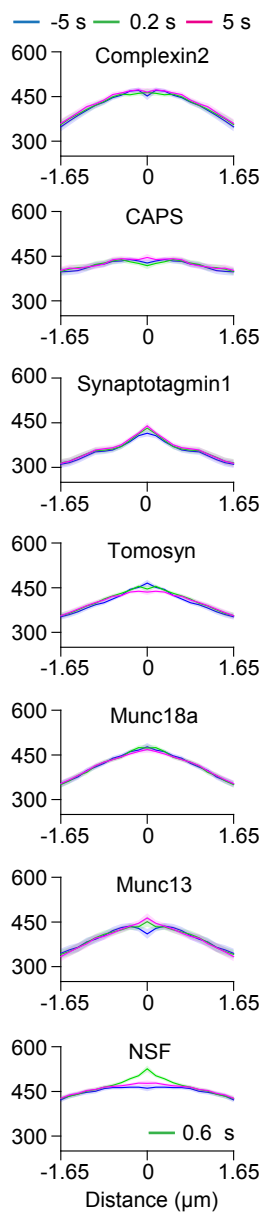
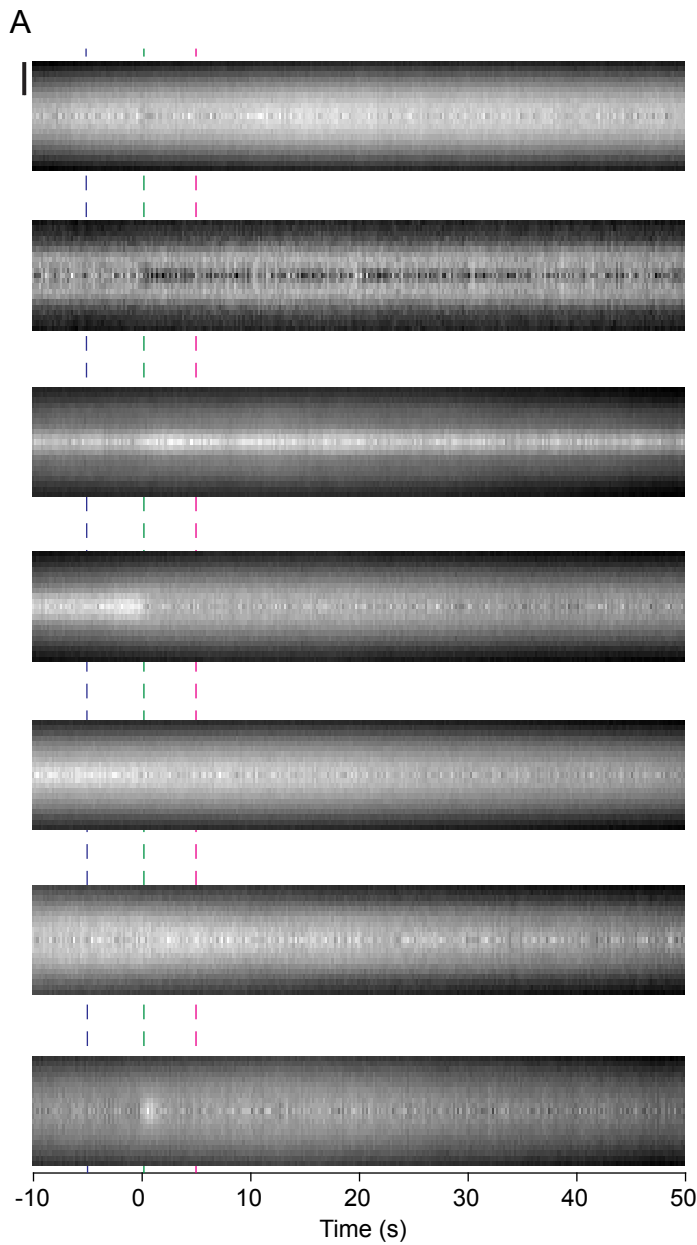
A

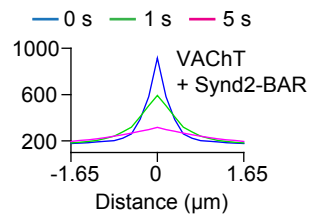
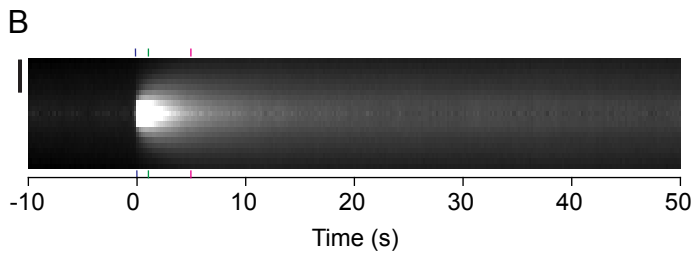
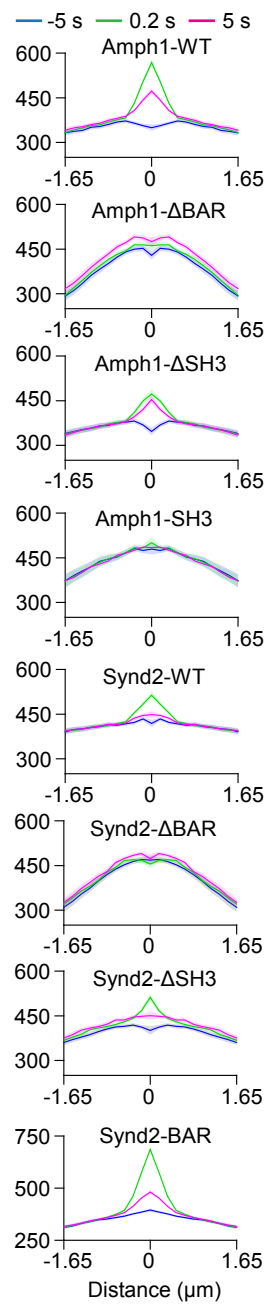
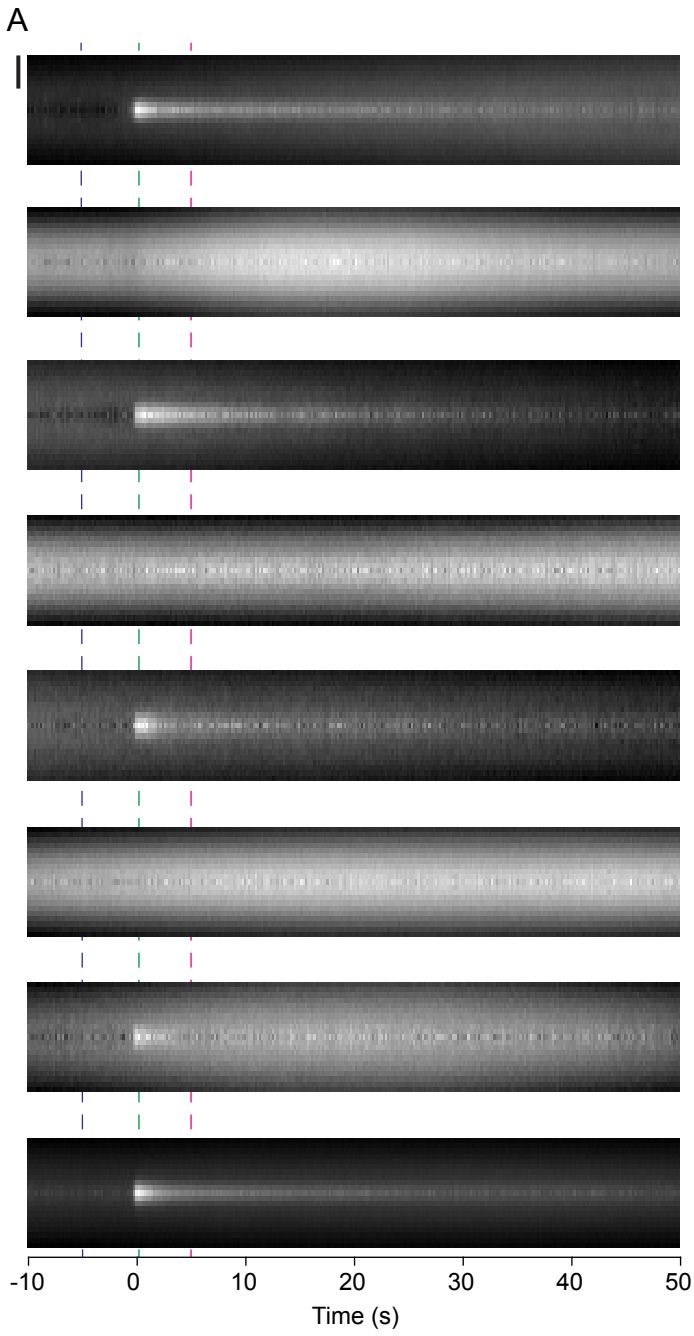


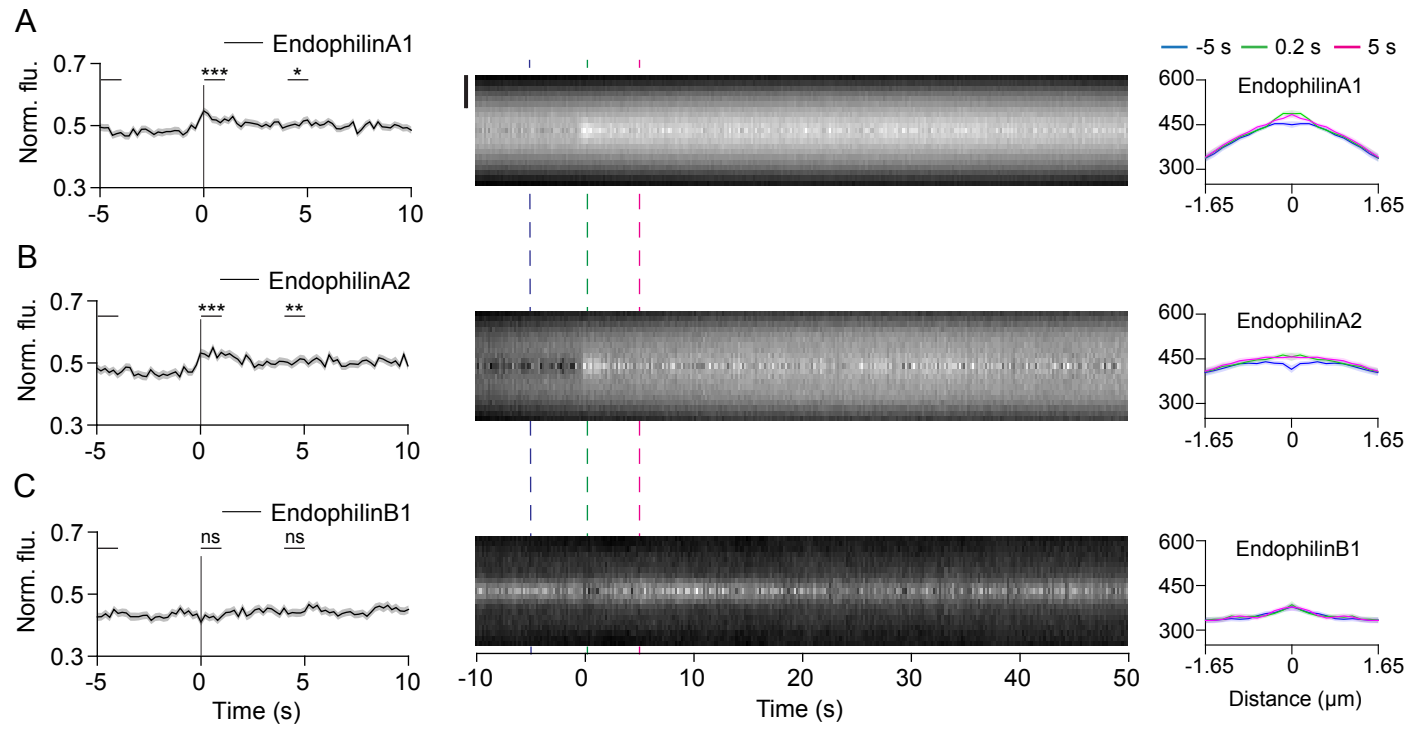
A

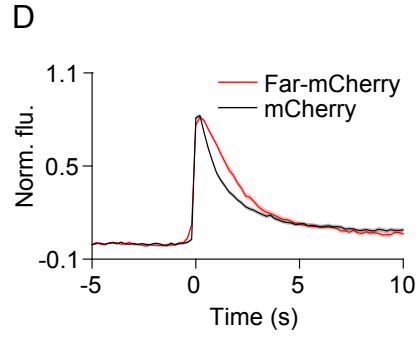
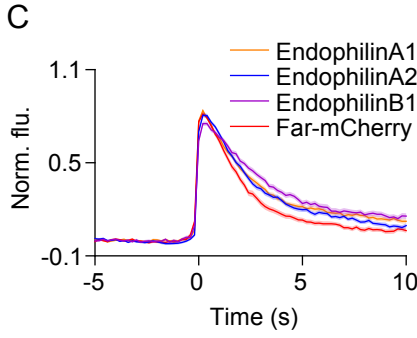
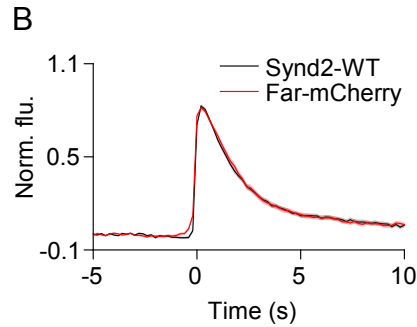
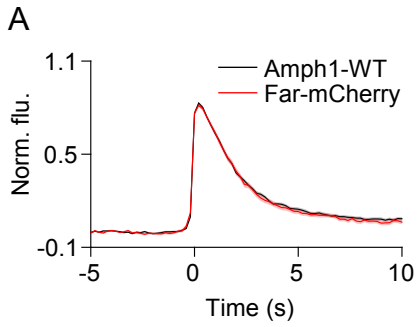


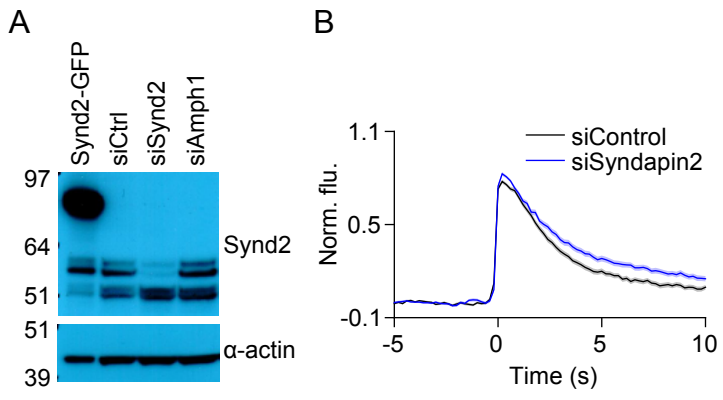


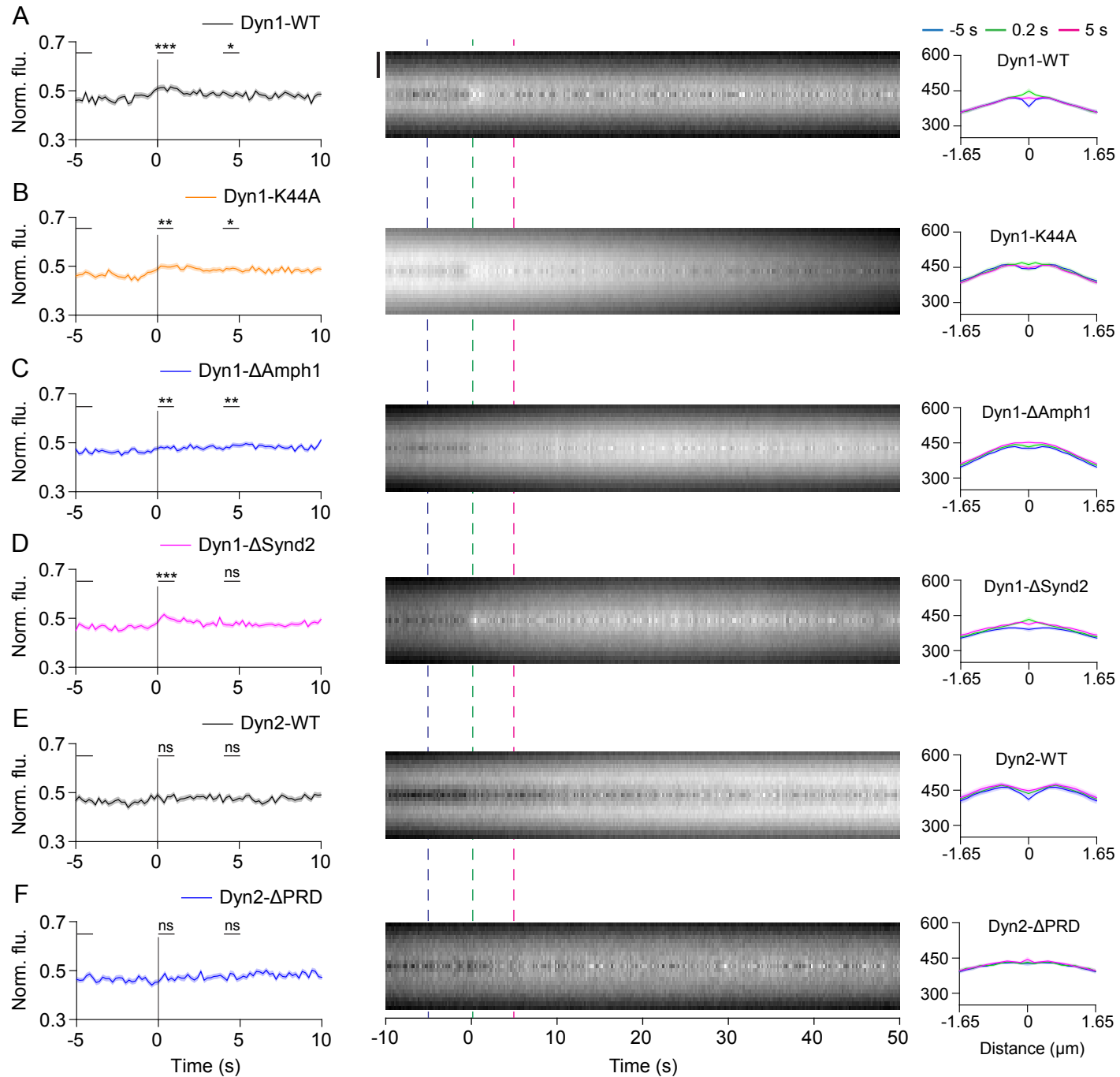


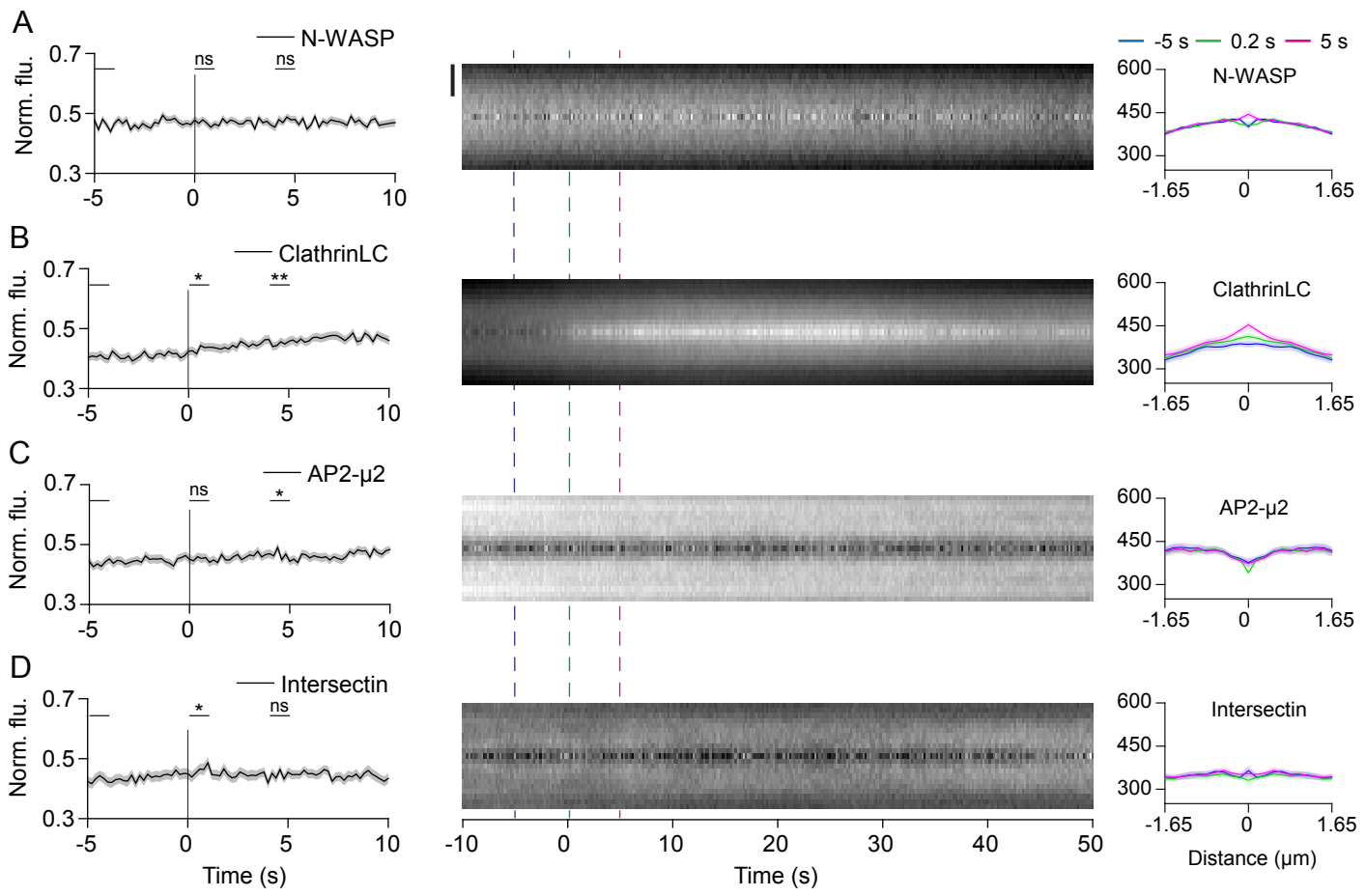


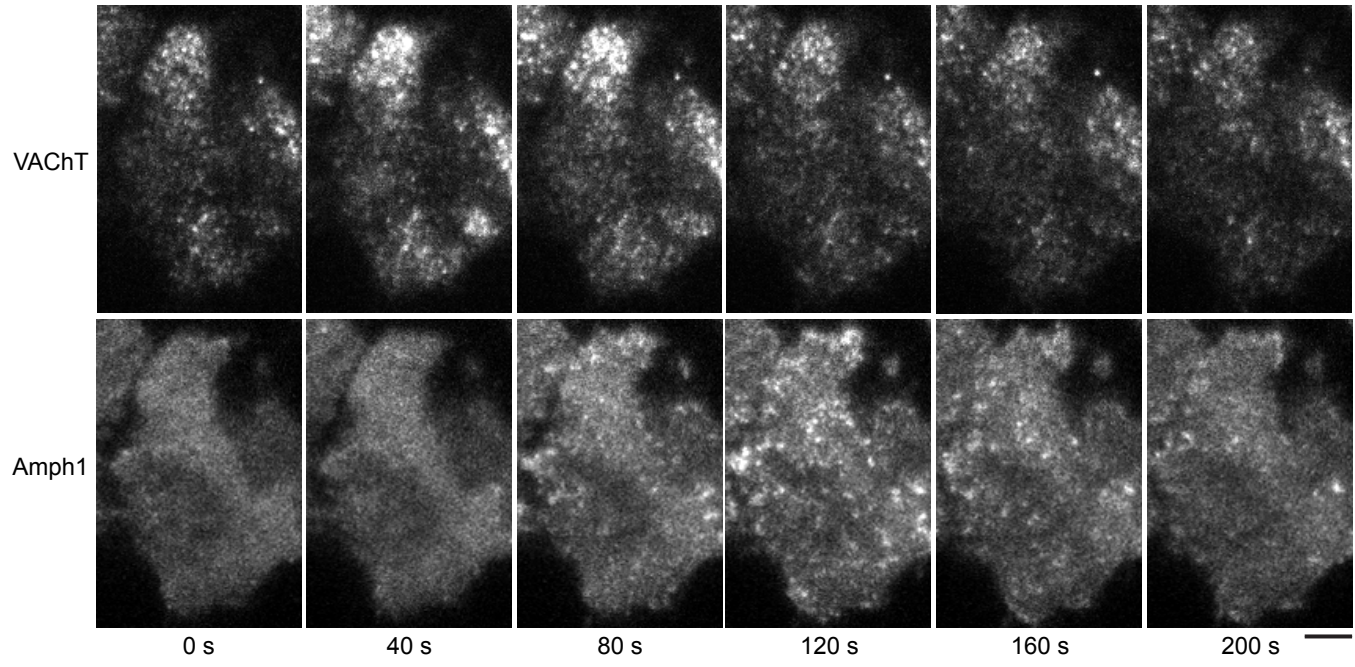










A**B**